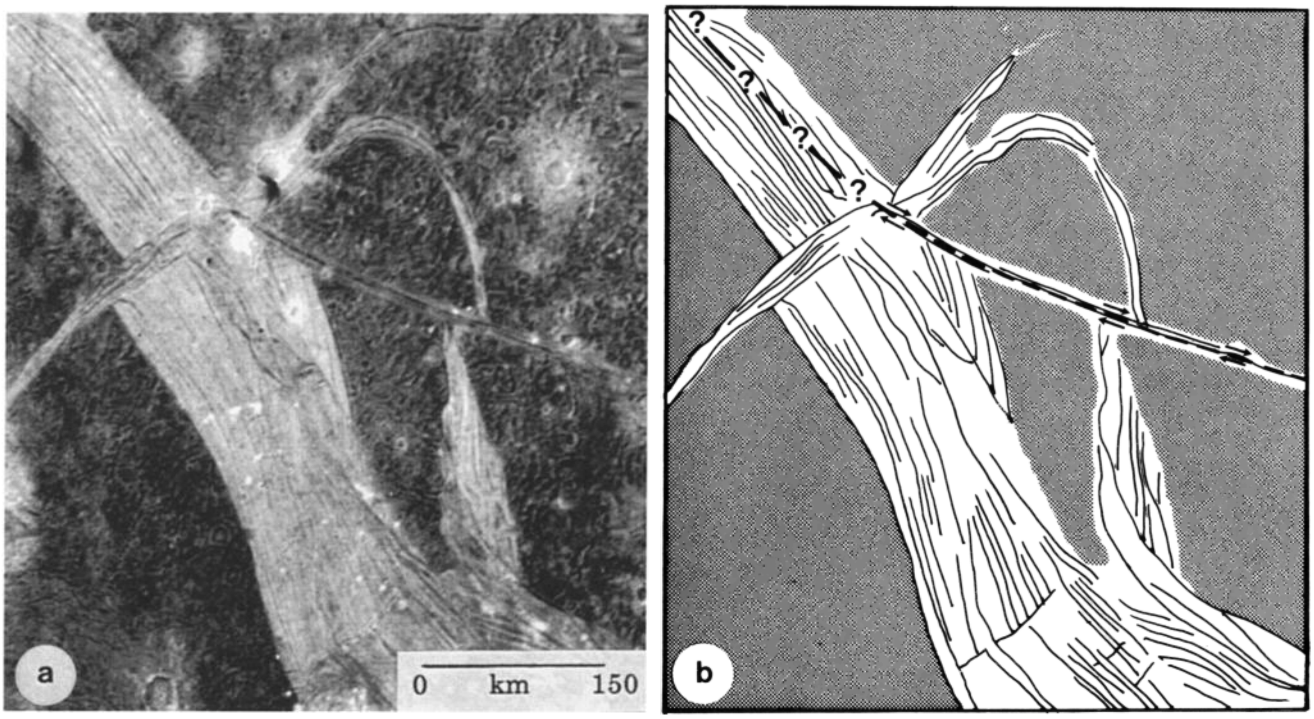

Fig. 15. (*a*) The right-laterally offset, curvilinear groove lane east of Tiamat Sulcus. North is up. (Voyager 2 image 20635.56, centered near 4°S,202°W.) (*b*) Structural map of same area. Grooves or troughs are shown in fine lines. The proposed strike-slip fault is shown as a heavy dashed line, and senses of offset are shown by arrows.

and are shown in Figure 4 as "C" and "C'," respectively. Lineament I continues to the east of 140°W where it becomes indistinguishable from lineament II, as a second major linear discontinuity in regional groove orientation (Figure 8). To the north of the lineament, grooves are east-northeast oriented and orthogonal to the arcuate furrows of Galileo Regio (area 1). To the south of the lineament, grooves are predominantly northwest-oriented and parallel to the arcuate furrows of central Marius Regio (area 3). These groove orientations form a high oblique angle, and are shown in Figure 4 as "D" and "D'," respectively.

The hypothesis of 500 km of left-lateral shear across lineament I predicts that some regional discontinuities in groove orientation, such as those described above, may be the result of reuse of older furrows whose orientations were offset across the lineament. As another test for this hypothesis, removal of the proposed shear should restore "C" and "C'" to parallel orientations, and "D" and "D'" to orthogonal orientations. Figure 13 shows the relationships of the four trends once the shear is removed: "C" and "C'" now are almost parallel, and "D" and "D'" now are orthogonal. Structural continuity across lineament I has been restored. Thus the number of possible independent structural indicators of 500 km of left-lateral movement across lineament I is now brought to five: the westward component of the separations of furrow poles of areas 1 and 3, the two offset dark terrain structures, and the two discontinuities in regional groove orientation.

Origin of Minor Furrow Noncircularity

As was just stated, there are several independent lines of evidence for 500 km of left-lateral shear across lineament I, which could account for the westward component of the separation of furrow poles of Galileo Regio and central Marius Regio. As is seen in Figure 16*a*, removing this shear restores to concentricity the bulk of the system I arcuate furrows in the two areas. However, two significant occurrences of nonconcentric furrows remain. The first is in the extreme western part of central Marius Regio, 50°-60° of arc from the giant palimpsest. As *Schenk and McKinnon* [1987] have suggested, furrow concentricity may break down at comparable distances from the source of stress for furrow formation, possibly due to lithospheric inhomogeneity.

The second occurrence of non-concentric furrows is in geographically adjacent portions of southern Galileo Regio and northern central Marius Regio (arrows, Figure 16*a*), covering about 1.5×10^6 km^2 within southern Galileo Regio. The deviation from concentricity is systematic and of a counterclockwise sense. As a result, the furrows in the area of nonconcentricity in Galileo Regio have a high radius of curvature that can explain the southward component of the furrow-pole separation of Galileo Regio and central Marius Regio.

In this second occurrence of furrow non-concentricity, a possible specific cause of lithospheric inhomogeneity is identifiable. As is seen in Figure 16*b*, in their "restored" configuration the nonconcentric furrows align with small circles centered on the center of curvature of the older arcuate furrows in system III. Reuse of older, approximately concentric structures within system III thus emerges as a possible simple explanation for much of the deviation of system I arcuate furrows from circularity.

System I Radial Furrows

Examination of system I radial furrows provides an additional opportunity for testing different interpretations of the geology of the arcuate furrows: that the giant palimpsest in east-central Marius Regio is the true center of the system I arcuate furrows,